

POLITECNICO DI TORINO

DIMEAS – DEPARTMENT OF MECHANICAL AND AEROSPACE
ENGINEERING

Master's Degree thesis

DENSITY MEASUREMENT OF THE LOW GWP REFRIGERANT
(HCFO-1224yd) USING VTD



Academic Supervisor:

Prof. Vito Claudio Fericola

INRiM supervisors:

Dr. Lago Simona

Dr. Romeo Raffaella

Candidate:

Manikanta Garapati

S227992

Academic year 2021-2022

Acknowledgement

I would like to thank my esteemed supervisor Prof. Vito Claudio Fericola, Senior researcher at INRIM, for allowing me to carry out this project and for his invaluable advice and patience throughout my thesis study.

My gratitude extends to my external supervisor Dr. Simona Lago, Senior researcher of INRIM for her invaluable supervision, professionalism, treasured support, and plentiful experience that have encouraged me all the time during the thesis work. I also thank Dr. Giuliano Albo Paolo Alberto and Dr. Cavuoto Giuseppe for their kind help and technical support in my study.

I am indebted to Dr. Raffella Romeo, INRIM Researcher for her continued guidance, immense knowledge, answering with unfailing patience, reading my numerous revisions, and helped make some sense of the confusion. I also want to thank you for the attention you gave to the thesis throughout that time.

Last, but not least, my warm and heartfelt thanks go to my parents and friends for the tremendous support and hope they had given to me in the past few years. Without that hope, this study would not have been possible. Thank you all for the strength you gave me. I love you all!

Abstract

The purpose of this experimental thesis is to determine the density of new refrigerant fluid from the family of hydrochlorofluoro-olefins (HCFOs). The necessity to characterize this sort of fluid, known commercially as the fluorinated gas AMOLEA™ R1224yd (cis-1-chloro-2,3,3,3- tetrafluoropropene), is due to its very low environmental impact, as indicated by a low global warming index. Following the publication of current rules that impose severe limits on the use of non-environmentally friendly fluids, interest in this form of refrigerant has surged. The aim of the thesis is to provide density measurements of this new refrigerant, necessary for its complete thermodynamic characterization, also due to the limited number of experimental measurements currently available in the literature.

This thesis work begins with a brief history of refrigerant fluids and the many factors that led to its discovery and use. We then go on to discuss the different issues associated with the environmental impact of ozone depletion and the greenhouse effect, which are responsible for our planet's slow but progressive warming.

The theory and description of the Anton-Paar 512P vibrating tube densimeter are then presented, as well as a description of how it operates and is used. The technique used to load the refrigerant fluid to be examined into the system is then described, as how the data are obtained and evaluated.

A total of 89 compressed liquid density data for R1224yd were acquired along 9 isotherms with temperature steps of 10 K between 273 K and 353 K. and in the pressure range from 1 MPa to 35 MPa in approximate steps of 5 MPa. Measurements were obtained with an expanded relative uncertainty of 0.05 %. Finally, the experimental densities were compared with the data available in the literature.

Contents

List of Figures	2
List of Tables	2
1. Introduction	3
1.1. History of refrigerants.....	4
1.2. Environmental Impact.....	7
1.2.1. Ozone layer	7
1.2.2. Global Warming	10
1.3. Regulation and Legalization	12
1.4. Type of Refrigerants.....	14
1.5. Classification of Refrigerants	14
1.5.1. Fluorinated refrigerants	14
1.6. Fluorinated derivatives of propene	16
1.7. The fluid R1224yd(Z)	18
2. Measuring Principle	20
3. Experimental setup	22
3.1. High pressure circuit and temperature control	23
4. Experimental Procedure	24
4.1. Preliminary cleaning and system tightness assessment	25
4.2. Vacuum calibration	25
4.3. Calibrating the system using bi-distilled water.....	26
4.4. Charge of the refrigerant fluid and process for determining the period of oscillation	27
4.5. Data collection and processing	28
5. Evaluation of the uncertainty	29
6. Density data and Results.....	31
7. Conclusion.....	36
8. Bibliography	37
9. Appendix	39

List of Figures

Figure 1 Development of Refrigerants [1].	4
Figure 2: Surface affected by the ozone hole in Antarctica (October 2016) [5].	9
Figure 3 : Average ozone hole area for multiple years from early September to mid-October [6].	9
Figure 4 : Life cycle climate performance components [8].	11
Figure 5 : Stereoisomers for R1234ye. On the left the R1234ye (E) while on the right the R1234ye (Z) [4].	17
Figure 6 : Structural formula for HCFO R-1224yd(Z) [13].	19
Figure 7 : Schematic representation of the experimental apparatus used for measuring densities [15].	22
Figure 8 : Diagram of the Anton-Paar 512P vibrating tube densimeter [5].	23
Figure 9 : R1224yd compressed liquid densities as a function of pressure along isotherms ranging 273.15 K to 353.15 K.	31
Figure 10 : Deviations of R1224yd(Z) experimental densities from the values of REFPROP [18] as a function of pressure for temperatures ranging 273.15 K to 353.15 K.	34
Figure 11 : Distribution in the (T, p) plane.	35
Figure 12 : Deviations from Fedele et al. (2020) data and experimental compressed liquid density as a function of pressure for temperatures ranging 273.15 K to 353.15 K. [19].	35

List of Tables

Table 1 : Generations of Refrigerants[1].	6
Table 2 : The proposed suffixes for the propene isomers.	17
Table 3 : Properties of R1224yd [12].	18
Table 4 : Density uncertainty budget considering a coverage factor k=2.	30
Table 5 : Compressed liquid density experimental data for R1224yd(Z), with the percentage deviations from the values (ρ_{rprop}) implemented by REFPROP.	32

1. Introduction

Refrigerant is the fluid used for heat transfer in a refrigerating system that absorbs heat during evaporation from the region of low temperature and pressure, and releases heat during condensation at a region of higher temperature and pressure. Refrigerants are the working medium in refrigerating systems that evaporate by absorbing heat from the region to be cooled, resulting in a cooling effect.

Refrigeration is the technique of obtaining and maintaining a temperature lower than that of the surroundings in order to cool a product or area to the appropriate temperature. Consumable food products are preserved by being kept at low temperatures, which is one of the most significant uses of refrigeration. Refrigeration systems are also widely employed to provide thermal comfort to humans through air conditioning. Air conditioning is the treatment of air to control its temperature, moisture content, cleanliness, odour, and circulation at the same time, as required by inhabitants or products in the space. The history of refrigeration goes back many centuries and is rooted in human needs for comfort and food.

Throughout history, refrigerant development has occurred for a variety of causes, including safety, stability, durability, and economic, or environmental concerns, resulting in new research and equipment improvements in terms of safety and efficiency. The refrigerants are categorized into generations, which are explained further below [1].

1.1. History of refrigerants

Mechanical refrigeration began in the early nineteenth century and was characterised by the use of natural refrigerants. The first refrigerants considered for use in mechanical refrigeration systems were water and air. In his invention for the vapour compression refrigeration system in 1834, Perkins offered ethyl ether as the working fluid. The Perkins system was a closed circuit that included all the contemporary vapour compression system components, including the compressor, condenser, expansion device, and evaporator.

When the refrigeration system was developing between 1830 and 1930, ammonia, carbon dioxide, sulphur dioxide, ethers, hydrocarbons, and air were utilized as refrigerants. In 1878, methyl chloride was used as a refrigerant for the first time. These are referred to as first-generation refrigerants. The first-generation refrigerants were chosen based on availability and what worked. These refrigerants were extremely flammable, toxic, and reactive [1].

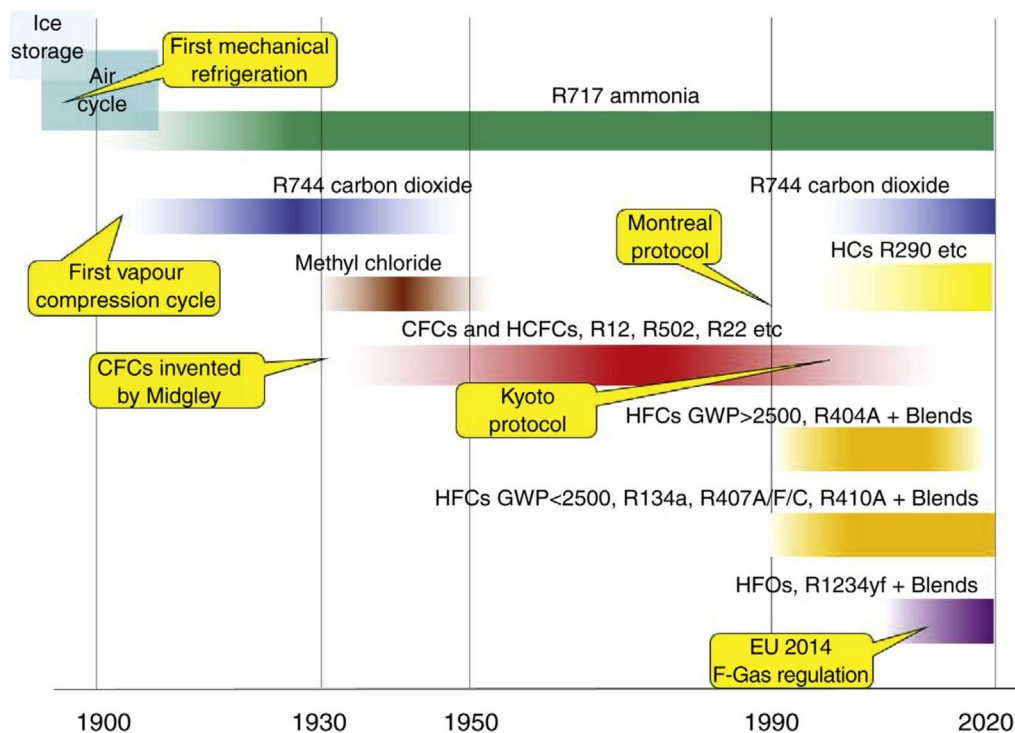


Figure 1 Development of Refrigerants [1].

In the early 12th century, chlorofluorocarbons (CFCs) overtook traditional refrigerants as shown in Figure 1. In 1928, Midgely and his colleagues conducted study to find a stable refrigerant that was neither toxic nor flammable. They choose R-12, dichlorodifluoromethane, as the suitable compound. R-12 was first commercially produced in 1931, followed by R-11 in 1932 and R-13 for low temperature applications in 1945 [1].

Starting in the 1950s, chlorofluorocarbons (CFCs), hydro chlorofluorocarbons (R-22) and zeotropic combination R-502 dominated the second generation of refrigerants. These refrigerants dominated the second half of the 20th century. The only natural refrigerant that remained popular in industrial applications was ammonia.

Researchers Roland and Molina predicted in 1974 that ozone in the stratosphere would be catalytically destroyed by HFC emissions, harming Earth's atmosphere. The prediction was proven in 1985 by measurements demonstrating the destruction of the ozone layer over Antarctica [1]. The Montreal Protocol, signed in 1987, established limits on CFC production and consumption. The Montreal Protocol's first phase was to switch from CFCs to HCFCs due to HCFCs ozone depletion. As a result, a range of HFCs and their derivatives were produced to fulfil the requirements of refrigeration applications. The focus was on reduced servicing and refrigerant emissions during service and disposal. This grade of refrigerant was classified as third generation. The Kyoto Protocol was developed in 1994 as a tangible implementing tool to decrease emissions under the United Nations Framework Convention on Climate Change (UNFCCC). The use of ozone-depleting substances is being reduced, and efforts are being made by both industrialized and developing nations to improve the controls outlined in the Protocol. Since HCFCs and HFCs only contribute around 2% of the overall global warming, therefore, these are on a schedule to be phased out by 2030 [2].

The higher atmospheric lifetime and global warming index directly depend on the number of fluorine atoms in HFCs. As a result, HFCs have come under scrutiny for their impact to greenhouse gas emissions. Therefore, they are being replaced by HFOs. Table 1 lists the development and generation of refrigerants.

Table 1 : Generations of Refrigerants[1].

Generation	Year	Refrigerants
1 st	1830-1930	R-744, R-717, R-764, R-170, R-40
2 nd	1931-1990	R-11, R-12, R-114, R-113
	1936	R-22, R-15, R-502
	1943	Mixture of R-11, R-12
	1949	R-500
	1975	Mixture of R-12, R-13
3 rd	1990- 2010	R-32, R-134A,R-404A, R-508A
4 th	2010 onwards	R-1270, R-1261,R-1252, R-1234YF,R-1224yd,
		R-1225, R-1216, R-1234

HFOs are unsaturated organic compounds made up of hydrogen, fluorine, and carbon. They have a carbon-carbon double bond, which is a significant feature that contributes to their low global warming. These synthetic refrigerants (HFOs) are being developed as fourth-generation refrigerants, with 0.1 % of the GWP of HFCs and several useful properties such as short survival periods when exposed to the atmosphere (i.e., low atmospheric lifetimes), low boiling points, excellent physicochemical properties, and high vapor pressures at room temperature. They are, therefore considered to be the best substitutes for HFCs [1].

1.2. Environmental Impact

1.2.1. Ozone layer

Ozone (O_3) is a significantly less stable triatomic type of oxygen (O_2). It is a blue gas that exists in low concentrations in the atmosphere. The ozone layer in the stratosphere prevents most of the sun's harmful ultraviolet (UV) rays from reaching the earth's surface.

A group of British scientists reported the results of a series of atmospheric measurements over Antarctica in 1985. The measurements lasted several years and revealed that when the Sun reappeared on the horizon after the long austral night (i.e., at the end of September, early October in our hemisphere), the amount of ozone in the upper atmosphere was substantially reduced [3].

The conclusion was later confirmed by a study of satellite data collected in the years preceding these most previous studies, which revealed an even more alarming condition than could be deduced from ground measurements. Following the occurrence, it was determined that the weakening of the ozone layer grew over time, known as "ozone hole".

Following that, an ozone layer depletion was discovered in a tiny location at the North Pole, over the Arctic Sea, which could lead to the emergence of another hole.

The phenomena are simply the most visible aspect of the general and progressive drop in ozone levels in the stratosphere. The issue is critical because a decrease in the ozone shielding effect leads to an increase in UV rays reaching the Earth's surface. Excessive exposure to these rays is linked to an increased risk of skin cancer in humans, which is caused by mutations in the DNA of epithelial cells. Ultraviolet radiation can also partially hinder plant photosynthesis, slowing growth and, in the case of cultivated plants, lowering yields. UV rays can also reduce the photosynthetic activity of phytoplankton situated at the bottom of the food chain, generating a substantial imbalance in ocean ecosystems.

The presence of a vast number of chemical compounds capable of destroying ozone in the atmosphere is certainly responsible for the continual and gradual depletion of ozone in the stratosphere. These compounds are also known as

ODS, Ozone Depleting Substances (substances that destroy ozone). ODS are normally very stable in the troposphere and degrade mainly because to the severe action of ultraviolet radiation in the stratosphere, when they break, chlorine and bromine atoms are released causing damage to the ozone layer.

To get a quantitative understanding of the impact of ODS compounds, the ozone depleting potential (ODP) was defined, which is an index that relates to the amount of ozone depletion caused by an ODS compound. To be more precise, ODP is defined by the quantity of chlorine and bromine atoms in the molecule from the compound's atmospheric "life" (the total time spent in the atmosphere, which can range from a few months to thousands of years), and the specific mechanisms involved in its degradation. ODP can be described as relation between the amount of chemical compound that impact the ozone to the impact caused by CFC-11 having the same mass as the substance under consideration [4]. Thus, the ODP is defined as:

$$ODP = \frac{(\Delta O_3)}{(\Delta O_3)_{CFC-11}}$$

Once the true impact of CFCs on ozone depletion was evident, governments approved regulations prohibiting the use of CFCs and replacing them with shorter-lived alternative species (HFCs and HCFCs), which had to be gradually phased out over time, allowing for a more rapid recovery of the ozone layer.

In 2016, the size and depth of the ozone hole above Antarctica were not exceptional. Ozone levels have stabilized, as expected, but full recovery will take decades.

Figure 2 shows the Antarctic ozone hole on October 1, 2016, as observed by the Ozone Monitoring Instrument (OMI) on NASA's Aura satellite. The ozone layer hit its average annual minimum concentration of 114 Dobson Units on that day. In comparison, the ozone layer hit a minimum of 101 Dobson Units in 2015. Long before the Antarctic ozone hole formed, typical ozone concentrations above the South Pole varied between 260 and 320 Dobson Units. In 2016, the area of the ozone hole peaked on September 28, 2016, at around 23 million square kilometres (8.9 million square miles) [5].

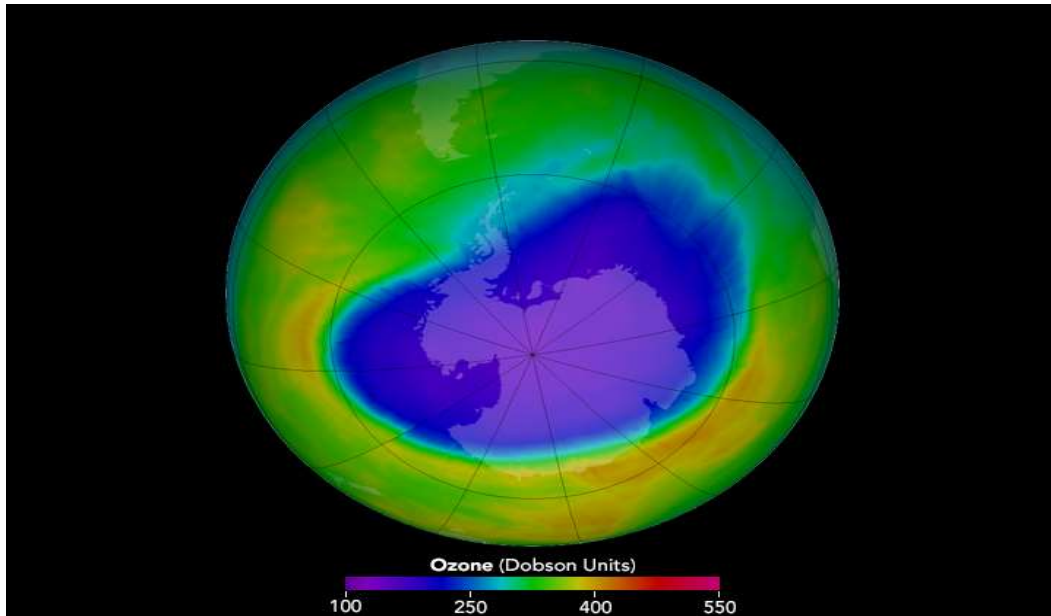


Figure 2: Surface affected by the ozone hole in Antarctica (October 2016) [5].

NASA satellite scans in 2021 showed that the ozone hole had widened to a maximum of 9.6 million square miles (24.8 million square kilometres), This year, scientists recorded the lowest total-column ozone value of 102 Dobson Units on Oct. 7, the 8th-lowest since 1986.

As shown in Figure 3, while the ozone hole in Antarctica in 2021 is greater than average, it is significantly lower than ozone holes in the late 1990s and early 2000s [6].

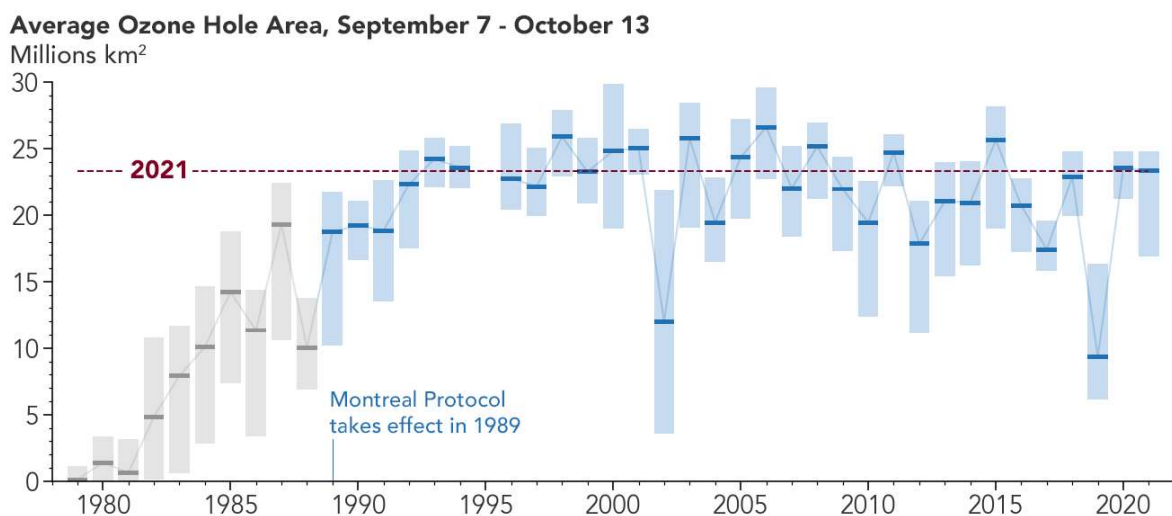


Figure 3 : Average ozone hole area for multiple years from early September to mid-October [6].

1.2.2. Global Warming

Global warming also known as the greenhouse effect, the phenomenon of increasing average air temperatures near the earth's surface to levels above natural levels. Since mid- 20th century the climate scientists have gathered circumstantial observations of various weather phenomena such as temperatures, precipitation, and storms of related impact on climate. These data indicate that Earth's climate has changed over almost every time phase since at least the beginning of the industrial revolution to extent of present day [7].

Most of the rays from the sun that reaches the earth are visible light, some of its energy is absorbed by the surface of earth after entering through the atmosphere and this process is converted into thermal energy. The earth emits the infrared radiation and contributes to a slow and progressive warming of the planet. The radiation is significantly absorbed by the greenhouse gases present in the atmosphere. Some of the gases are ozone (O₃), Carbon dioxide (CO₂), water vapor (H₂O), methane (CH₄), nitrogen dioxide (N₂O) and some of refrigerant fluids such as hydrofluorocarbons (HFCs), chlorofluorocarbons (CFCs) hydrochlorofluorocarbons (HCFCs), etc..

In recent years, the increase in concentration of these greenhouse gases in earth's atmosphere has affected the temperature of the earth's surface caused by human activities. The studies and research of this effect has led to establish a direct correlation between increase in temperature and the increase in greenhouse gases.

The Global Warming Potential (GWP) index has been introduced in order to evaluate the contribution of any refrigerants on its global warming potential. The GWP index is set by the Intergovernmental Panel on Climate Change (IPCC) to measure the contribution of solar thermal radiation that is absorbed by the greenhouse gas over certain period (e.g., 100 years) with reference to the absorption of an equal quantity of CO₂. It is defined as:

$$GWP = \frac{\int_0^t NFR dt}{\int_0^t NFR(CO_2) dt}$$

Where, NFR is the infrared absorption coefficient of the observed gas.

Constant efforts and studies are focused on search of low GWP fluids thanks to the simplicity in identifying the direct emission of the refrigerant, but it is also important to recognize the indirect effects such as in stationary A/C applications.

In January 2012, the International Institute of Refrigeration (IIR) formed a Working Group to investigate the merits of the Life Cycle Climate Performance (LCCP) methodology. Life Cycle Climate Performance is an index by which HVAC&R systems can be evaluated for their global warming impact over the course of their lifetime. It is calculated as the sum of direct and indirect emissions generated over the lifetime of the system from “cradle to grave.” Figure 4 shows how LCCP is considered throughout the entire life cycle weighing both direct and indirect effects [8].

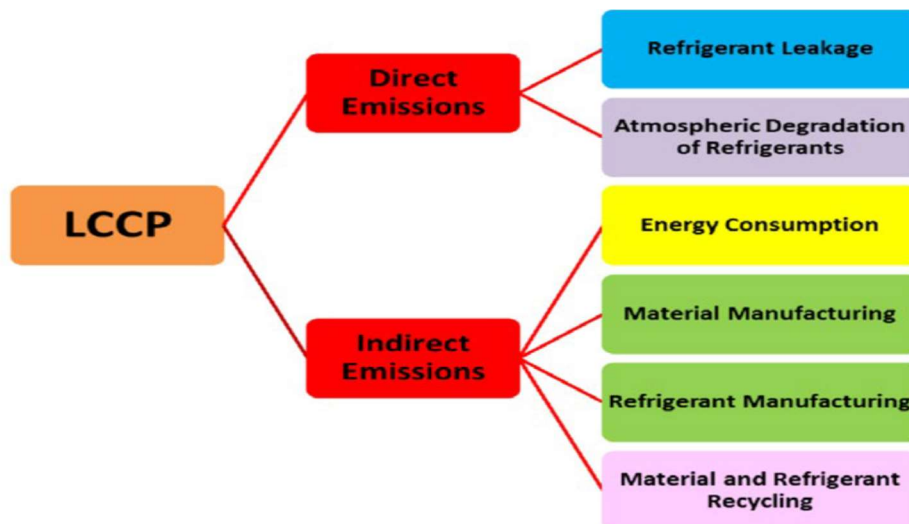


Figure 4 : Life cycle climate performance components [8].

1.3. Regulation and Legalization

Montreal Protocol and Kyoto Protocol are the international legal references relating to production and use of substances that are harmful to ozone layer and responsible for greenhouse effect regarding use of refrigeration fluids.

The Montreal protocol was the first international agreement signed in 1987, by industrialized countries to limit and then eliminate the production and consumption of nearly 100 man-made chemicals referred to as Ozone Depleting Substance (ODS) harmful to stratosphere ozone.

The Montreal protocol phases down the production and consumption of the different ODS in a step wise manner, with various plans for developed and developing countries. Under this agreement, all members have specific commitment related to phase out of different group of ODS, like annual reporting of data, national licensing system to control ODS imports and exports, control of ODS trade and other matters. This treaty expands over time of new technical, economical, and scientific developments, and it continues to be altered and adjusted.

HCFCs are used all over the world in many applications like air conditioning, refrigeration, and foam applications, but they are being phased out since they deplete the ozone layer under the Montreal protocol. HCFCs are both ODS and greenhouse gases and they are 2000 times more potent than CO₂ in terms of GWP. Because of this, in September 2007 the members decided to accelerate their schedule to phase out HCFCs completely by 2020 for developed countries, and developing countries agreed to start phaseout process in 2013 and follows stepwise reduction to complete phaseout by 2030.

To date, the Montreal protocol have phased out 98% of ODS globally compared to 1990 levels, from 1990-2010 the control measures are estimated to have decrease greenhouse gas emissions by around 135 gigatons of CO₂, which is 11 gigatons a year [9].

The Kyoto protocol was approved on 11th December 1997, but came into force on 16th February 2005, over 192 parties are following this protocol. The Kyoto protocol (first commitment period) sets emission reduction targets for 37 industrialized countries and to the European union. Compared to year 1990

levels these targets add up to 5% emission reduction by five years period 2008-2012.

For the second commitment period Doha amendment to Kyoto protocol was started in 2013 and lasting until 2020. Over 147 countries showed their instrument of acceptance as of 28th October 2020, the amendment came into force on 31st December 2020 with an entry threshold of 144 instruments of acceptance was achieved [10].

The Kyoto protocol allows for the use of market mechanism, namely Flexible mechanism, the main aspect is the clean Development mechanism. The main aim of this mechanism is to reduce emissions at the lowest possible cost. To date, 174 countries and a regional economic integration organization have started the procedure for ratification, 61.6 % of global greenhouse gases are from these countries. India and China, which have approved to this protocol, are not required to reduce CO₂ emission under this agreement, because of their relatively large population. Many other developing countries with India and China are exempted from the Kyoto protocol because they are not among the main contributors to greenhouse gas emissions during the period of industrialization. Since the planet has been polluted by industrialized countries and only in the last decade by developing countries, the reduction of emissions must be corresponding with a weight factor, which is calculated in relation to historical contribution of last two centuries. From this point of view, a new revised common agreement should be followed by every member for the betterment of planet.

1.4. Type of Refrigerants

Primary refrigerants are fluids that are used directly as working fluids, such as in vapour compression and vapour absorption refrigeration systems, these fluids produce refrigeration in compression or absorption systems by undergoing a phase transition process in the evaporator. Secondary refrigerants are liquids used to transmit heat energy from one site to another, these refrigerants are also known as brines and antifreezes.

1.5. Classification of Refrigerants

1.5.1. Fluorinated refrigerants

Fluorinated refrigerants are mostly responsible for ozone layer depletion and contribute to global warming. The interactions between the two phenomena are true, but they are extremely complex. The refrigerant classes are discussed below.

- CFCs (chlorofluorocarbons)

They are triatomic molecules composed of fluorine, chlorine, and carbon that are often formed through halogen exchange starting with chlorinated methane's and ethane's. They are stable, which allows them to easily reach the stratosphere. CFCs are used in a variety of applications due to their higher boiling temperatures and superior thermodynamic features such as low toxicity, flammability, and reactivity. CFCs are less flammable because they contain fewer C-H bonds, and their densities are larger than those of their comparable alkanes. At this point, its transformation causes it to contribute to the ozone layer's depletion.

- HCFC (hydro chlorofluorocarbon)

They are transitional compounds, which are molecules made up of carbon, chlorine, fluorine, and hydrogen. They are less stable than CFCs and hence destroy ozone to a lower amount. The inclusion of hydrogen atoms reduces their stability and gives them a shorter lifetime in the atmosphere, i.e., they are more likely to breakdown before reaching the ozone layer. From the 1960s through the mid-1990s, HCFC (Freon 22) was utilized in domestic air conditioners. Even while HCFCs are significantly better than CFCs at reducing ozone harm, they are still a significant greenhouse gas.

- HFC (hydro fluorocarbons)

They are substitution substances, which are molecules made up of carbon, fluorine, and hydrogen. They do not include chlorine and so do not contribute to the depletion of the ozone layer, in HFCs chlorine is totally replaced by hydrogen, resulting in almost zero ozone depletion. HFCs have adequate properties in terms of safety, efficiency, reliability, and availability which meet the needs of industry. Unfortunately, HFCs have high GWP (thousands of times greater than carbon dioxide) because of the presence of fluorine gases relative to other greenhouse gases.

- HFO (hydro fluoro-olefin)

HFOs include the same elements as HFCs, such as carbon, hydrogen, and fluorine, but they are unsaturated organic molecules therefore the suffix "olefin". HFOs now on the market are based on alkenes such as propene (e.g., HFO-1234yf or HFO-1234ze) and, in rare cases butene (e.g., HFO[1]1336mzz) or ethene (HFO-1132a). They have a double bond between two carbon atoms, just like their hydrocarbon parent. Because of the double bond, the molecules become less stable, resulting in fast breakdown in the atmosphere - within a few days as opposed to years or decades for HFCs [11].

1.6. Fluorinated derivatives of propene

The fluorinated derivatives of propene have a carbon-carbon double bond and are also known as olefins.

As a result, in addition to the designation R (for refrigerants), fluorinated propene derivatives can be designated by the prefixes HFO (hydrofluoro-olefin), HCFO (hydrochlorofluoro-olefin), HFA (hydrofluoro-alkene), or HFC (hydrofluoro-carbon).

The refrigerant classification is based on the ANSI / ASHRAE 34 standard "Designation and Safety Classification of Refrigerants." For the fluorinated isomers of propene, the designation consists of four digits followed by two or three letters.

The following points summarize the compound's chemical composition:

The first digit represents the number of double carbon bonds. The second digit represents the number of carbon atoms decreased by one. The third digit represents the number of hydrogen atoms increased by one. The fourth digit represents the number of fluorine atoms, and the letters represent the type of isomer obtained from the same formula.

The two additional letters distinguish the fluorinated isomers of propene. Table 2 summarizes the numbering scheme for the two additional letters that distinguish the fluorinated isomers of propene. The first additional letter refers to the central carbon replacement, the second letter refers to the terminal carbon substitution group of methylene.

Table 2 : The proposed suffixes for the propene isomers.

Central carbon replacement		Terminal carbon substitution group of methylene	
Substitution group	Letter	Substitution group	Letter
-Cl	<i>x</i>	=CCl ₂	<i>a</i>
-F	<i>y</i>	=CClF	<i>b</i>
-H	<i>z</i>	=CF ₂	<i>c</i>
		=CHCL	<i>d</i>
		=CHF	<i>e</i>
		=CH ₂	<i>f</i>

For some refrigerants the hydrogen and fluorine atoms are connected to the terminal carbon and can thus be positioned either across the carbon-carbon double bond from each of them (designated with an additional letter "E" from the German "entgegen" which means "against") or on the same side of the carbon-carbon double bond (designated with an additional letter "Z" from the German "zusammen" which means "together"). For example, Figure 5 shows the spatial arrangement of their atoms of R1234ye.

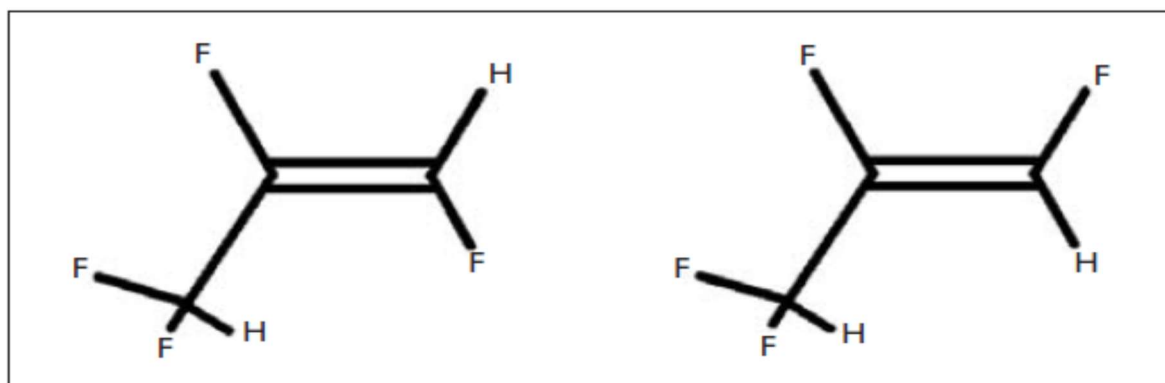


Figure 5 : Stereoisomers for R1234ye. On the left the R1234ye (E) while on the right the R1234ye (Z) [4].

1.7. The fluid R1224yd(Z)

Despite having chlorine in them, several of the new olefin-based refrigerants nonetheless manage to have almost little ozone depletion potential. These compounds are known as hydrochlorofluoro-olefins (HCFOs).

R1224yd has a very short atmospheric lifetime and consequently a very low GWP value because it contains a carbon-carbon double-bond with optimal positioning of F, C, and H atoms. Figure 6 shows the structural formula for the refrigerant 1224yd(Z). It is a non-flammable A1 refrigerant intended for use primarily in centrifugal chillers, binary cycle generators, and waste heat recovery heat pumps.

Table 3 : Properties of R1224yd [12].

Properties of R-1224yd(Z)	
Chemical name	(Z)-1-Chloro-2,3,3,3-Tetrafluoropropene
Molecular formula	(Z)-CF ₃ CF=CHCl
Molecular weight	148.5 g/mol
Normal boiling point (101.3kPa)	15 °C
Critical temperature	156 °C
Critical pressure	3.34 MPa
Critical density	527 kg/m ³
LC50	213,000 ppm
Atmospheric Lifetime	20days
ODP	0.00023
GWP	<1
Flammable range	None

HCFOs have an atmospheric life measured in days rather than years. Before reaching the stratosphere, HCFO refrigerants degrade rapidly in the atmosphere. This same property contributes to HCFO refrigerants lower global warming potential. HCFO-1224yd(Z) has a 21-day atmospheric life and almost no ozone depletion potential [12]. Table 3 shows molecular formula and properties of refrigerant 1224yd.

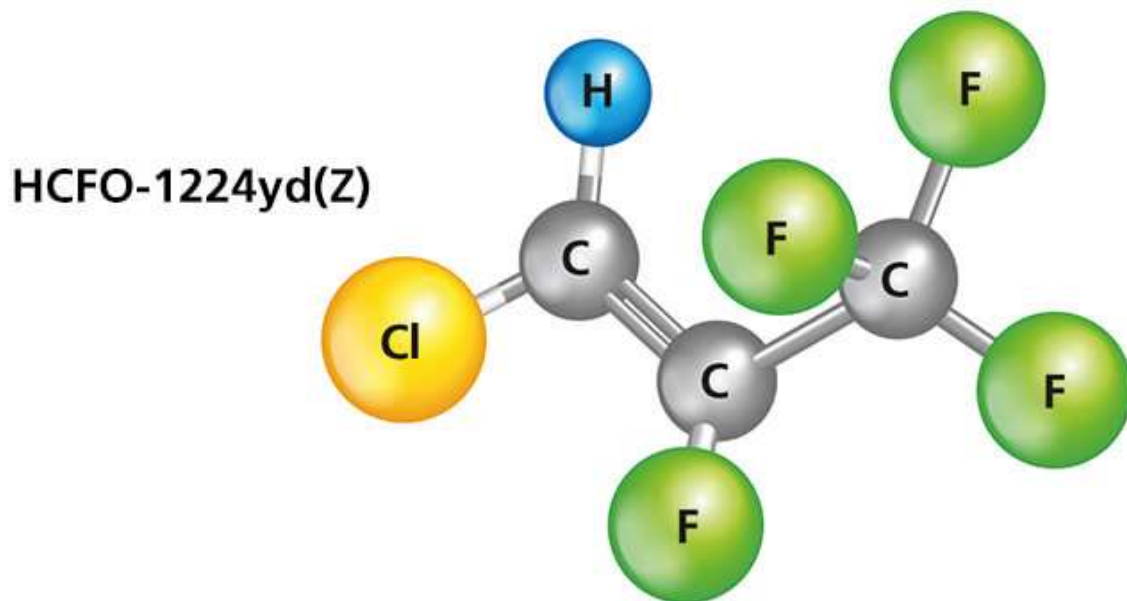


Figure 6 : Structural formula for HCFO R-1224yd(Z) [13].

2. Measuring Principle

The vibrating tube densimeter is one of the most used techniques to determine the density of pure fluids and mixtures, in a wide range of temperature and pressure. These are widely used for accurate measurements of fluids both in the gaseous and liquid phases, finding applications both in research and in industry. The major characteristics of these densimeters are their high precision, operational simplicity, and the small amount of sample volume required to record measurements.

The well-known principle of vibrating-tube densimeters is based on the theory of vibration and material deformation of mechanical oscillator concerning a U or V-shaped glass or metal tube (capillary) of constant volume filled with a fluid sample [14]. Stationary oscillations of the tube are maintained by the electromagnetic force, generated by means of a drive system acting on the tube. The input signal for the drive system is obtained from a pick-up system that converts mechanical oscillations of the tube into an electrical signal. Oscillations are close to the resonant frequency of the tube and are related to the density ρ of a fluid filled in. The resonant frequency f of a vibrating tube densimeter, as a function of the temperature T and pressure p , filled with a fluid, can be expressed as:

$$f(T, p) = \frac{1}{2\pi} \sqrt{\frac{k(T, p)}{m + V(T, p)\rho(T, p)}} \quad (1)$$

where k is the stiffness of the resonant element, m is the mass of the resonant glass or metal tube, and V is the volume of the fluid contained in the resonant element (inner volume of the capillary).

The densimeter is externally enclosed in a thermostatic chamber that allows the flow of a thermostatic fluid to maintain the proper temperature inside the measuring cell. The chamber contains an ampoule with a high thermal conductivity gas in which the "vibrating U-tube" is immersed. The oscillator must

be entirely filled with the sample substance with no voids or air bubbles to affect the data.

The tube is filled with the required amount of sample and is set to oscillate perpendicular to its plane exerting a suitable force on the tube by means of piezoelectric transducer, the sample changes the mass of the system and hence resonance frequency of the tube. Since the volume of U-shaped vibrating tube kept constant, there is a direct relationship between the period of the harmonic oscillation (τ) and the density of the liquid (ρ) contained in the tube. Therefore, considering Eq. 1, this relation is given by:

$$\rho(T, p) = A(T, p) \cdot \tau^2(T, p) - B(T, p) \quad (2)$$

where $A(T, p)$ and $B(T, p)$ are two apparatus parameters that consider both the volume and mass of the measuring cell in addition to its spring constant, defined as:

$$A = \frac{k(T, p)}{4\pi^2 V(T, p)}; \quad B = \frac{m}{V(T, p)} \quad (3)$$

3. Experimental setup

The experimental set-up for measuring density is demonstrated in Figure 7. It has been designed on an Anton Paar DMA 512P vibrating tube densimeter that is connected to an Anton Paar DMA 5000, which works as the control unit. The temperature of the measurement cell, which contains the vibrating tube, is controlled by circulating a thermostatic liquid pumped from a liquid bath thermostat.

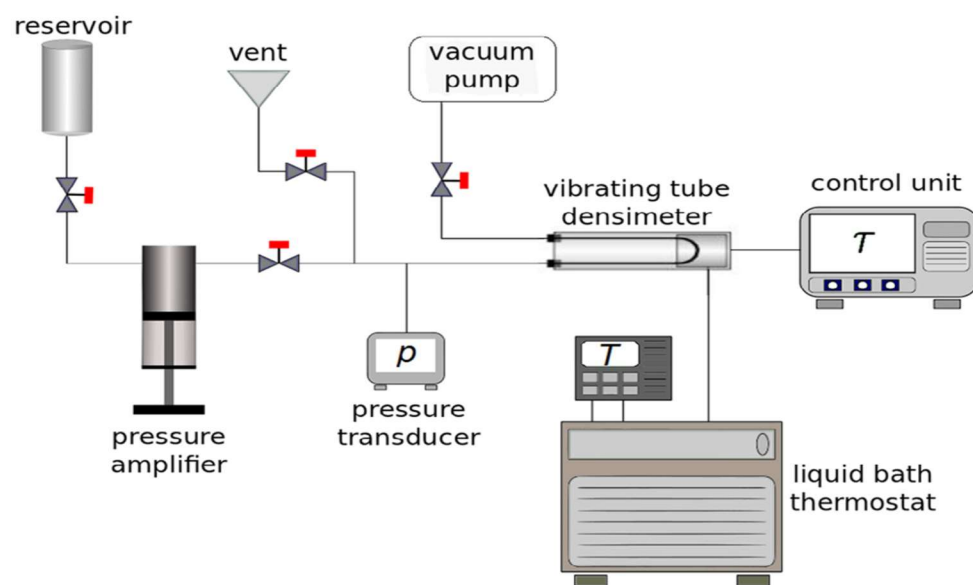


Figure 7 : Schematic representation of the experimental apparatus used for measuring densities [15].

The shut-off valve closes one side of the vibrating tube, while the other side is connected to a high-pressure circuit. This latter connects the measuring cell to the reservoir with the fluid under study at atmospheric pressure through a series of valves and is used to fill the capillary and increase the pressure inside it.

After the fluid under test has filled the measurement cell, pressure is controlled by regulating the valves by changing the volume of the hydraulic circuit. A pressure transducer with a full range scale of 70 MPa is used to monitor pressure.

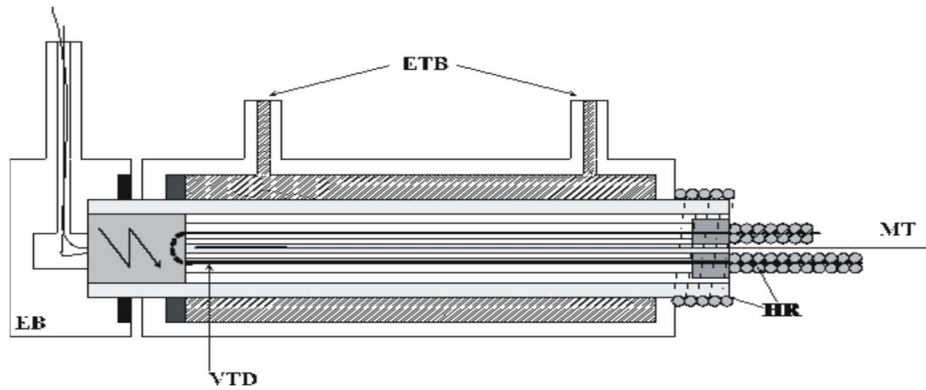


Figure 8 : Diagram of the Anton-Paar 512P vibrating tube densimeter [5].

Figure 8 shows the schematic representation of Anton Paar DMA512P densimeter, which was used to measure the oscillation period of refrigerant. It is constructed with elements that enable density measurements to be carried out under extreme pressure and temperature conditions.

3.1. High pressure circuit and temperature control

The high-pressure system consists of a system of valves and tube and a pressure control device. A pressure transducer was used to measure the pressure in the system, with an uncertainty of 0.03MPa, considering both the instrument resolution and the repeatability.

A liquid bath thermostatically controls the temperature of the measurement cell, which contains the vibrating tube. Heat losses through the vessel's wall and lid were further minimized by a 7 cm thick polystyrene insulating layer. The fluid in the bath was silicone oil. The temperature was maintained and controlled by a system comprised of the main thermostat with stability of ± 0.01 mK. This system was used to achieve ± 2 mK temperature stability in the bath over the entire working temperature range [16]. The temperature of the sample is measured with a PT100 platinum resistance thermometer and a thermometer readout. The temperature was obtained with an uncertainty of 0.03 K due to fit calibration, the resolution of the instrument, and the reading repeatability.

4. Experimental Procedure

To characterize and determine the instrument parameters indicated in Eq. (3), the vibrating periods of two reference fluids of known density must be determined. In order to simplify the calibration procedure, the period is usually measured in the evacuated tube, and charged with water. Following this approach, the unknown density can be calculated using the equation: [16].

$$\rho(T, p) = \rho_w(T, p) + \rho_{w1}(T, 1\text{MPa}) \frac{\tau^2(T, p) - \tau_w^2(T, p)}{\tau_{w1}^2(T, 1\text{MPa}) - \tau_0^2(T)} \quad (4)$$

where τ , τ_w , τ_{w1} , τ_0 are the measured periods related to the oscillation of the tube filled with the sample i.e., evacuated and charged with water. Eq. (4) improves the accuracy of the densities obtained in the liquid phase, lowering their uncertainty [16].

The following steps are involved in the experimental technique for estimating the unknown density i.e., density of refrigerant :

- Cleaning the system, checking the seals, and controlling the complete measurement system.
- Calibrating the vacuum system.
- Calibrating the system using bi-distilled water.
- Charging the refrigerant in the liquid state; and measuring the oscillation period of the densimeter.
- Recalibration with vacuum and water to verify calibration and regulate obtained data.

The details of each of the aforementioned steps are provided below.

4.1. Preliminary cleaning and system tightness assessment

Even if the system is cleaned and vacuumed after each measurement campaign, a pre-operational cleaning is essential to avoid unpleasant difficulties during the measurements.

The pipes and different mechanical connections are cleaned using acetone, and then the acetone and any remnants of the previously tested fluids are eliminated using a flow of pure nitrogen.

After this technique is completed, the system is tested for leaks by adding nitrogen and compressing it with syringe pumps. Nitrogen, with its small molecules compared to the other test fluids, is particularly ideal for testing system tightness since it is more susceptible to leaks through various sealing devices such as T-joints and joint fittings.

If any leaks are observed, it is essential to intervene by replacing gaskets, tightening connecting rings more tightly or in the worst-case scenario replacing them, which requires cutting the pipe and replacing the components that allow the seal.

4.2. Vacuum calibration

To determine the density of the sample fluid indirectly, it is necessary to know the calibration constants that allow to compare the oscillation period of the densimeter filled with sample refrigerant, with the period determined with the calibrating fluids.

To obtain the conditions required for the calibration with vacuum, a mechanical compressor is utilized, which allows for a vacuum level of roughly 0.08 kPa. The compressor is run for at least a couple of days to guarantee a level of vacuum enough to consider zero density within the experimental uncertainty, removing as much air as possible as well as any other molecules trapped in the densimeter or the rest of the system.

The vacuum was selected as the calibrating fluid because it is associated with a density of about 0 kg/m^3 and is valid for the lower limit of the range within which the density of the refrigerant to be examined must fall. The oscillation period of vacuum was measured in the temperature range from 273.15 K to 343.15 K,

along 6 isotherms, i.e., the same thermodynamic states over which the refrigerants are measured.

4.3. Calibrating the system using bi-distilled water

As a second fluid to complete the calibration procedure, bi-distilled water is used as a fluid of known density because thanks to its extreme purity it allows to obtain a known density value with the minimum value of uncertainty.

The density of the bi-distilled water is calculated using the equation of state for water, the IAPWS-95 formulation proposed by Wagner and Pruss [17].

A small cylinder with the water sample is connected to a vacuum compressor, in order to extract the air present inside circuit. Once the correct degree of vacuum is obtained, the cylinder is connected to the system.

Given enough time to return the system to vacuum after the unavoidable input of air during the bottle connection phase, the water is loaded by opening the main valve located in the lower part of the upside-down bottle. By opening the valve of the bottle, the water is introduced due to thrust action of atmospheric pressure which thus leads to completely fill U shaped tube of the densimeter. This prevents the entry of air which could alter the oscillation period of the tube.

During the water filling phase, the circuit's intermediate valve that separates the pumps from the densimeter and pressure gauge must be closed. Water molecules have the ability to stick to the walls of the ducts and devices through which they are made to flow, which influences their ease of cleaning.

Pure water oscillation period was recorded at temperatures ranging from 273.15 K to 343.15 K, along 8 isotherms, and at pressures ranging from 1 MPa to 35 MPa, i.e., the same thermodynamic states over which the refrigerant is measured.

This calibration is useful since the vibration period of the tube can vary slightly over time due to the stresses it is subjected to and the age of the components. It also accounts for the effects of pressure and temperature on the tube, which have three effects on the resonant frequency:

- As the temperature rises, the tube expands, lowering the resonance frequency.
- With rising temperature, the tube becomes less stiff, and the resonance frequency falls.
- With rising pressure, the radius and length of the tube rise, and the resonance frequency increases.

4.4. Charge of the refrigerant fluid and process for determining the period of oscillation

After measuring the oscillation periods for the calibration fluids, the system must be cleaned again. After removing the water from the system with a nitrogen flow, the system was cleaned with acetone, which drags the remaining water molecules and allows their total removal. The acetone is evacuated and evaporated by a subsequent flow of nitrogen and increasing the temperature. The system is then placed under vacuum for a day.

Finally, the charge of the refrigerant fluid to be researched can begin, i.e., the fluid R1224yd (cis-1-chloro-2,3,3,3- tetrafluoropropene, $\text{CF}_3\text{CF}=\text{CHCl}$). The refrigerant is enclosed within a pressure vessel which has been degassed (method of removing dissolved gasses from liquids).

The refrigerant cylinder is attached to the system, and once the connection is confirmed to be secure, the cylinder valve opens to begin the introduction of the refrigerant, which causes a minor dip. The refrigerant cylinder can be disconnected at the end of the charging process to begin the measurements.

Nine isotherms were measured at temperatures ranging from 273.15 K to 353.15 K, with steps of 10 K between subsequent readings, and pressure is adjusted for each isotherm in steps of 5 MPa, ranging from 35 MPa to 1 MPa. At the completion of the measurements, the system must be emptied and cleaned with acetone and a nitrogen flow, then vacuumed to ensure effective cleaning.

4.5. Data collection and processing

The equation for determining density is implemented using the GNU Octave (GUI) software. GNU Octave, version 5.2.0, is a high-level language designed primarily for numerical computations. It provides a simple command-line interface for numerically solving linear and nonlinear problems, as well as executing other numerical experiments in a language that is mainly compatible with MATLAB.

By selecting the data of the fluid as output, a DAT document acquired including the density values of the fluid as well as the relevant temperature, pressure, and period of oscillation data.

5. Evaluation of the uncertainty

The relative expanded uncertainty of density was estimated as a function of the measured quantities to determine density: pure water density ρ_w , ρ_{w1} , vibrating periods τ_w , τ_{w1} , τ_0 , temperature T , and pressure p :

$$\rho = \rho(\rho_w, \rho_{w1}, \tau_w, \tau_{w1}, \tau_0, T, p) \quad (5)$$

As a result, the uncertainty propagation indicated below was used to determine the relative uncertainty of the refrigerant density.

$$\begin{aligned} \frac{u(\rho)}{\rho} = \frac{1}{\rho} \left[\left(\frac{\partial \rho}{\partial \rho_w} \right)^2 u^2(\rho_w) + \left(\frac{\partial \rho}{\partial \rho_{w1}} \right)^2 u^2(\rho_{w1}) + \left(\frac{\partial \rho}{\partial \tau} \right)^2 u^2(\tau) + \right. \\ \left. \left(\frac{\partial \rho}{\partial \tau_{w1}} \right)^2 u^2(\tau_{w1}) + \left(\frac{\partial \rho}{\partial \tau_w} \right)^2 u^2(\tau_w) + \left(\frac{\partial \rho}{\partial \tau_0} \right)^2 u^2(\tau_0) + \left(\frac{\partial \rho}{\partial T} \right)^2 u^2(T) + \right. \\ \left. \left(\frac{\partial \rho}{\partial p} \right)^2 u^2(p) \right]^{0.5} \quad (6) \end{aligned}$$

The relative uncertainty can be reformulated as follows by calculating the derivatives of Eq. (6) from Eq. (4), giving a clear expression of the sensitivity coefficients.

$$\begin{aligned} \frac{u(\rho)}{\rho} = \frac{1}{\rho} \left[\left(\frac{\tau^2 - \tau_w^2}{\tau_{w1}^2 - \tau_0^2} \right)^2 u^2(\rho_{w1}) + \left(\frac{2\tau\rho_{w1}}{\tau_{w1}^2 - \tau_0^2} \right)^2 u^2(\tau) + \left(\frac{2\rho_{w1}\tau_{w1}(\tau^2 - \tau_w^2)}{(\tau_{w1}^2 - \tau_0^2)^2} \right)^2 u^2(\tau_{w1}) + \right. \\ \left. \left(\frac{-2\tau_w\rho_{w1}}{\tau_{w1}^2 - \tau_0^2} \right)^2 u^2(\tau_w) + \left(\frac{-2\rho_{w1}\tau_0(\tau^2 - \tau_w^2)}{(\tau_{w1}^2 - \tau_0^2)^2} \right)^2 u^2(\tau_0) + \left(\frac{\partial \rho}{\partial T} \right)^2 u^2(T) + \right. \\ \left. \left(\frac{\partial \rho}{\partial p} \right)^2 u^2(p) + u^2(\rho_w) \right]^{0.5} \quad (7) \end{aligned}$$

In Table 4 there are all the sources and the associated uncertainties that contribute to the density uncertainty. The uncertainty for the vibration period is $0.1 \mu\text{s}$, which corresponds to the repeatability of 10 readings at each measuring thermodynamic state. The temperature measurements by the PT100 resistance thermometer have an uncertainty of 0.03 K due to fit calibration, instrument resolution, and reading repeatability. The pressure transducer uncertainty is 0.03 MPa considering both the instrument resolution and repeatability.

Table 4 : Density uncertainty budget considering a coverage factor $k=2$.

Uncertainty source	Relative magnitude %
water density	0.001
oscillation period	0.02
temperature	0.007
pressure	0.006
Relative expanded uncertainty (k=2)	0.05

The relative uncertainty in the measurements of density is calculated using Eq. (6) with a coverage factor of 2. The resulting uncertainty is 0.05% at the confidence level of 95%. Table 5 provides the sources of uncertainty, the values of the sensitivity coefficients shown in Eq. (7). All the sensitivity coefficients were calculated considering the worst-case scenario, i.e., using the data that maximized the sensitivity coefficient values. It is observed that the major contribution to the density uncertainty is due to the vibrating period measurement.

6. Density data and Results

This section presents the data from the study of the refrigerant R1224yd in liquid phase. The experimental data of R1224yd(Z),- in the temperature range between 273 K and 353 K and pressure varying from 1 MPa to 35MPa are reported in Table 5. Figure 9 shows a plot of the experimental densities calculated by Eq. (4) as a function of pressure along nine isotherms. Figure 10 shows the deviations of experimental densities from the values provided by the REFPROP database [18] as a function of pressure for all the measured temperatures.

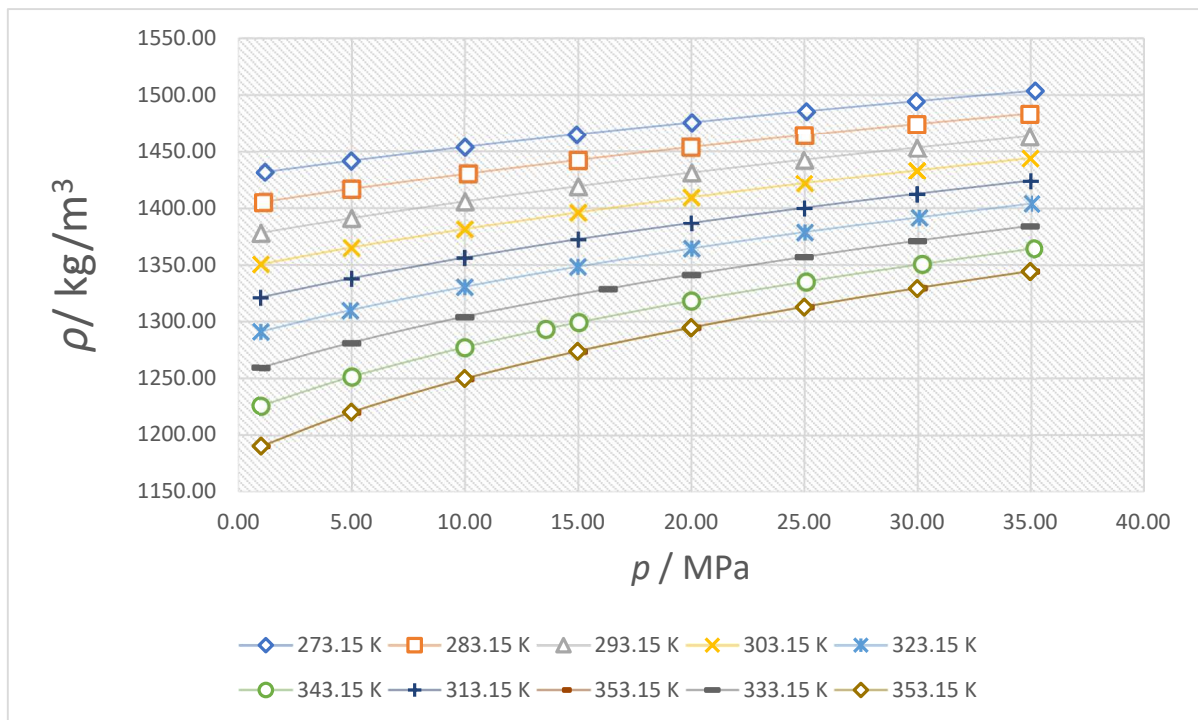


Figure 9 : R1224yd compressed liquid densities as a function of pressure along isotherms ranging 273.15 K to 353.15 K.

Table 5 : Compressed liquid density experimental data for R1224yd(Z), with the percentage deviations from the values (ρ_{rprop}) implemented by REFPROP.

T/K	p /MPa	$\rho_{exp}/\text{kg}\cdot\text{m}^{-3}$	$\rho_{rprop}/\text{kg}\cdot\text{m}^{-3}$	$10^2 \cdot (\rho_{exp} - \rho_{rprop}) / \rho_{rprop}$
273.16	1.19	1431.593	1430.715	0.06
273.15	4.99	1441.457	1440.752	0.05
273.16	10.01	1453.602	1452.963	0.04
273.16	14.94	1464.735	1464.110	0.04
273.18	20.04	1475.320	1474.779	0.04
273.16	25.10	1485.396	1484.794	0.04
273.17	29.96	1494.354	1493.849	0.03
273.16	35.22	1503.623	1503.145	0.03
283.16	1.12	1405.137	1404.768	0.03
283.17	5.01	1416.497	1416.109	0.03
283.15	10.15	1430.153	1429.883	0.02
283.14	15.01	1442.130	1441.782	0.02
283.14	19.99	1453.514	1453.086	0.03
283.14	25.00	1464.114	1463.714	0.03
283.15	29.99	1473.971	1473.603	0.03
283.30	34.99	1483.128	1482.714	0.03
293.15	1.00	1377.822	1377.881	0.00
293.15	5.01	1390.846	1390.927	-0.01
293.15	10.01	1405.536	1405.654	-0.01
293.15	15.00	1418.857	1418.979	-0.01
293.15	20.01	1431.114	1431.243	-0.01
293.16	24.99	1442.434	1442.571	-0.01
293.15	30.01	1453.118	1453.242	-0.01
293.15	34.98	1463.183	1463.193	0.00
303.15	1.01	1350.357	1350.414	0.00
303.15	5.00	1364.980	1365.042	0.00
303.15	10.00	1381.323	1381.308	0.00
303.15	10.01	1381.323	1381.323	0.00
303.15	15.00	1395.986	1395.871	0.01
303.15	15.01	1395.983	1395.880	0.01
303.15	20.00	1409.353	1409.147	0.01
303.15	20.00	1409.365	1409.143	0.02
303.15	25.01	1421.676	1421.376	0.02
303.15	30.01	1433.124	1432.749	0.03
303.16	30.01	1433.112	1432.731	0.03
303.16	35.01	1443.878	1443.384	0.03
323.15	1.01	1291.120	1292.031	-0.07
323.13	4.94	1309.805	1310.685	-0.07
323.16	10.00	1330.439	1331.040	-0.05
323.16	15.00	1348.179	1348.558	-0.03
323.15	20.01	1364.167	1364.250	-0.01
323.14	25.00	1378.544	1378.445	0.01

323.15	30.06	1391.570	1391.567	0.00
323.16	35.06	1403.784	1403.616	0.01
343.16	1.01	1225.917	1227.279	-0.11
343.15	5.01	1251.414	1252.743	-0.11
343.16	10.00	1277.313	1278.203	-0.07
343.14	13.58	1293.229	1293.903	-0.05
343.14	15.04	1299.237	1299.814	-0.04
343.15	20.00	1318.108	1318.187	-0.01
343.16	25.07	1335.001	1334.915	0.01
343.15	30.18	1350.395	1350.187	0.02
343.15	35.15	1364.227	1363.762	0.03
313.16	0.99	1321.152	1321.767	-0.05
313.16	5.01	1337.837	1338.385	-0.04
313.15	9.99	1356.172	1356.423	-0.02
313.16	10.01	1356.060	1356.452	-0.03
313.15	15.00	1372.317	1372.432	-0.01
313.22	20.02	1386.627	1386.710	-0.01
313.20	25.02	1400.031	1399.920	0.01
313.14	30.00	1412.411	1412.169	0.02
313.16	30.01	1412.405	1412.129	0.02
313.15	35.02	1423.898	1423.509	0.03
353.15	1.01	1190.295	1191.525	-0.10
353.14	5.01	1220.346	1221.684	-0.11
353.15	10.00	1249.720	1250.735	-0.08
353.16	15.00	1273.928	1274.442	-0.04
353.15	20.02	1294.763	1294.793	0.00
353.15	25.01	1312.985	1312.611	0.03
353.16	30.00	1329.395	1328.592	0.06
353.16	35.00	1344.316	1343.197	0.08
333.15	1.00	1259.522	1260.577	-0.08
333.16	5.00	1281.321	1282.359	-0.08
333.15	10.00	1304.195	1304.982	-0.06
333.15	16.32	1328.563	1329.016	-0.03
333.15	20.01	1341.222	1341.375	-0.01
333.16	25.00	1356.813	1356.657	0.01
333.15	30.01	1371.053	1370.626	0.03
333.15	35.00	1384.114	1383.466	0.05
353.16	1.00	1190.058	1191.415	-0.11
353.14	5.00	1220.162	1221.615	-0.12
353.15	10.00	1249.694	1250.722	-0.08
353.15	15.00	1273.876	1274.444	-0.04
353.16	20.01	1294.609	1294.731	-0.01
353.16	20.01	1294.623	1294.750	-0.01
353.15	25.01	1312.892	1312.599	0.02
353.15	30.01	1329.371	1328.620	0.06
353.17	34.99	1344.246	1343.151	0.08

353.14	35.00	1344.290	1343.221	0.08
--------	-------	----------	----------	------

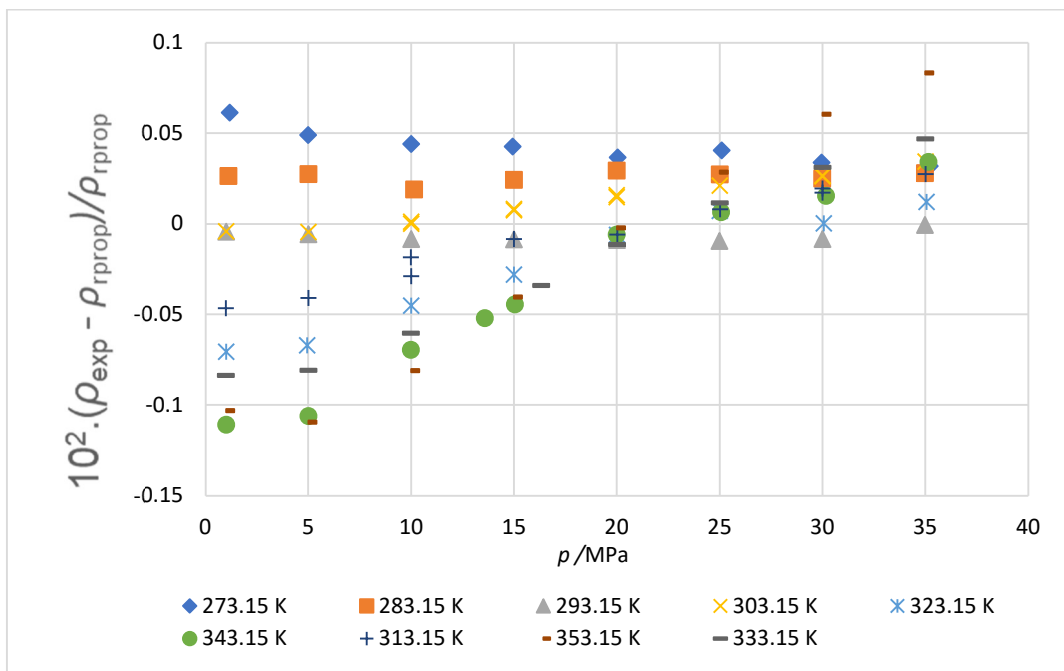


Figure 10 : Deviations of R1224yd(Z) experimental densities from the values of REFPROP [18] as a function of pressure for temperatures ranging 273.15 K to 353.15 K.

For the density values of the R1224yd, the proposed model presents an uncertainty of 0.05% considering a coverage factor $k=2$. By comparing the data acquired with REFPROP the deviation obtained a maximum value of $\pm 0.12\%$, observing the percentage deviation for the various isotherms, it is noted that the highest value is obtained for the isotherms at 353.15 K.

Furthermore, the experimental data were compared to the other experimental densities available in the literature, provided by Fedele et al. (2020) [19]. The distribution in the (T, p) plane of the present data and the data from Fedele et al. (2020) is shown in figure 11. The measurements carried out by Fedele et al. (2020), also using a vibrating tube densimeter, for temperatures from 283.25 K to 363.15 K and pressure from close to saturation pressure up to 35 MPa. The deviation of this values and from Fedele et al. densities are shown in Figure 12 as a function of pressure for temperatures ranging 273.15 K to 353.15 K and the deviation obtained a maximum value of $\pm 0.13\%$.

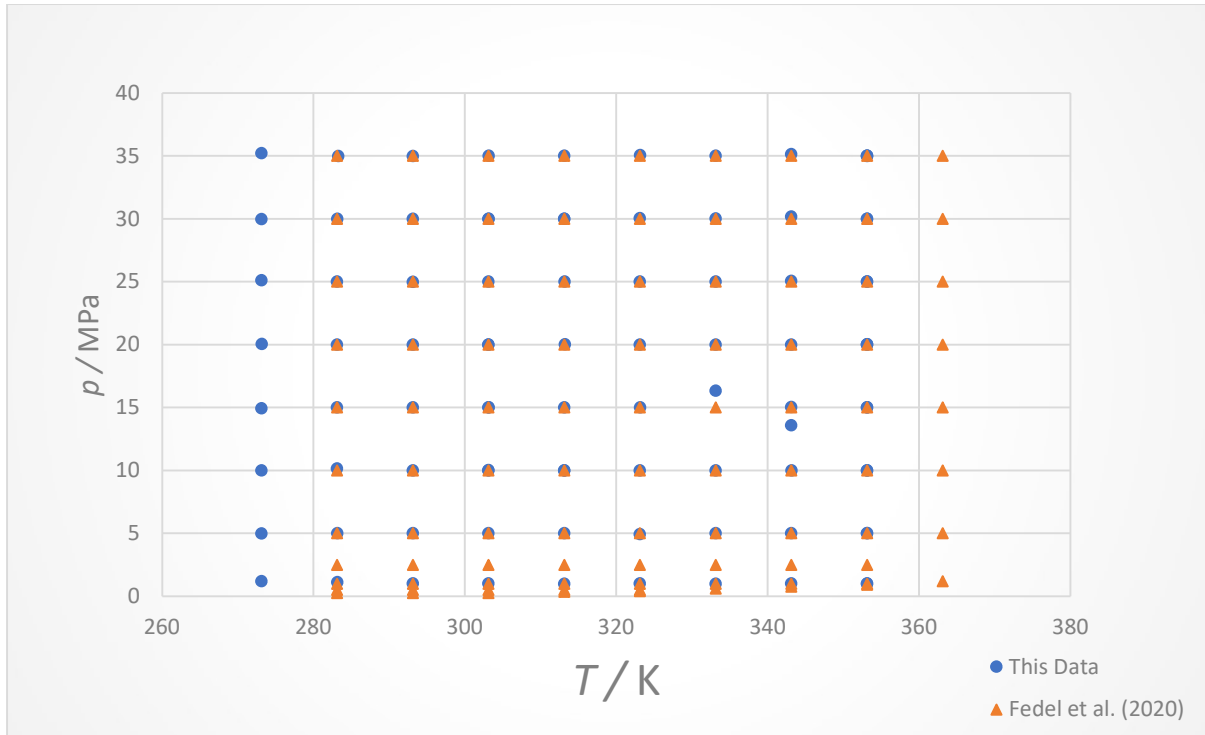


Figure 11 : Distribution in the (T, p) plane.

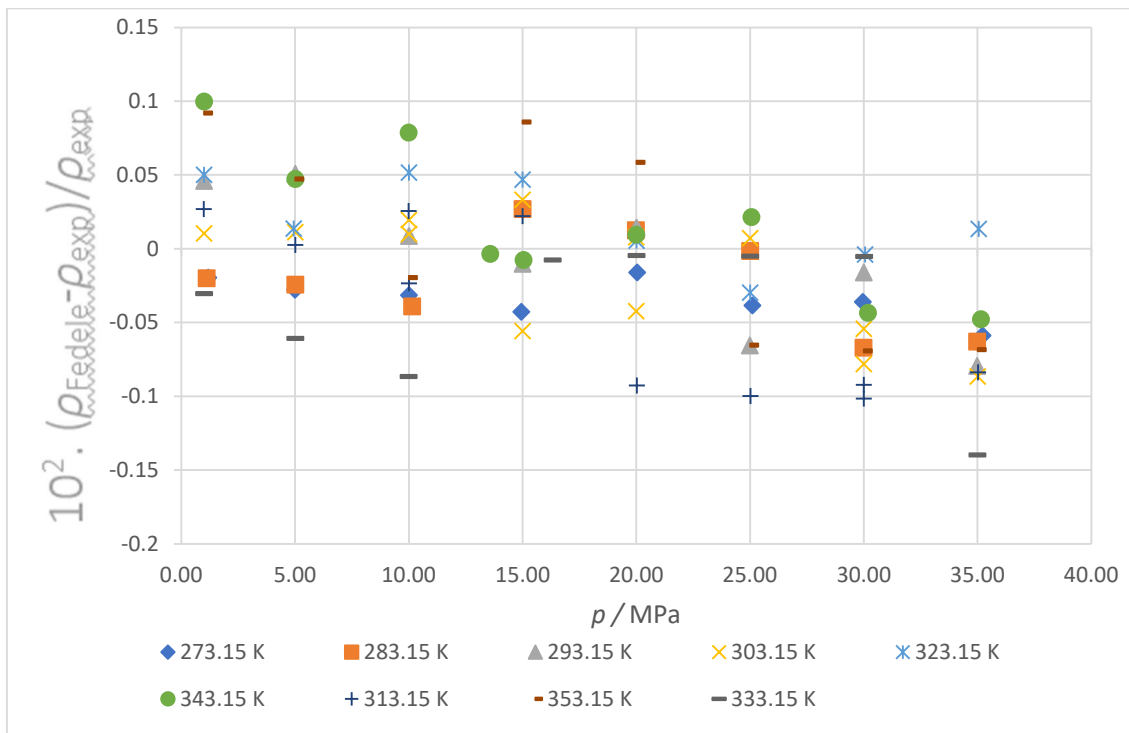


Figure 12 : Deviations from Fedele et al. (2020) data and experimental compressed liquid density as a function of pressure for temperatures ranging 273.15 K to 353.15 K. [19]

7. Conclusion

This experimental study arose with the aim to enhance data on a new type of refrigerant fluid, belonging to the class of HCFOs, i.e., the fourth generation of refrigerants, which have a minimal greenhouse effect and near zero ozone destructive power.

Currently, the most studied refrigerants of this type are R1224yd. This fluid is considered a valid substitute for HFC-245fa in high-temperature heat pumps or centrifugal chillers and applications such as Organic Rankine Cycles(ORC).

Since there is ongoing and growing interest in environmentally friendly, alternative refrigerants possessing low and ultra-low GWP values and because of the need for experimental data, in particular of density, due to the scarce amount of measurements available in the literature, the thesis publicly provides density measurements of refrigerant (Z)-1-Chloro-2,3,3,3,-Tetrafluoropropane, i.e., R1224yd(Z).

The density measurements were taken using a vibrating tube densimeter (Anton Paar DMA512P), calibrated by means of two reference fluids, i.e., vacuum and bi-distilled water. R1224yd(Z) in the compressed liquid state was measured over the pressure range from 1 MPa to 35 MPa, along 9 isotherms: 273.15 K, 283.15 K, 293.15 K, 303.15 K, 313.15 K, 323.15 K, 333.15 K, 343.15 K, 353.15 K. The measurements were carried out with a relative expanded uncertainty of 0.016%.

The experimental densities were compared with the literature data using the REFPROP database [18].

The measured values were also compared with the measured densities of Fedele et al. (2020) [20], with both datasets demonstrating good agreement over the entire T - p range and all deviations are within $\pm 0.13\%$.

8. Bibliography

1. [S. K. Bandey, A study on Refrigerants, *CSVТУ Research Journal on Engineering and Technology*, Vol. 8\(1\), 21-30, 2019.](#)
2. [P. Arora, G. Seshadri, A. K. Tyagi, Fourth-generation refrigerant: HFO 1234yf, *Current Science*, 115,1497, 2018.](#)
3. [M. R. Schoeberl and J. M. Rodriguez, The Rise and Fall of Dynamical Theories of the Ozone Hole, *Twenty Years of Ozone Decline*, 263-272, Springer, Dordrecht, 2009.](#)
4. [M. Securo, Analisi Sperimentale della Densità di Refrigeranti a basso Impatto Ambientale, Tesi di Laurea, Università degli Studi di Padova, 2013.](#)
5. [NASA, "Ozone Hole 2016, and a Historic Climate Agreement, October 1, 2016.](#)
6. [NASA, "2021 Antarctic Ozone Hole 13th-Largest, Will Persist into November, October 27, 2021.](#)
7. [M. E. Mann, H. Selin, "Global warming". Encyclopedia Britannica, Jan 2022. <https://www.britannica.com/science/global-warming>.](#)
8. [Y. Hwang, Harmonization of Life Cycle Climate Performance Methodology, 32nd Informatory Note on refrigeration technologies, 20, 2016.](#)
9. [UNEP, The Montreal Protocol, Environmental rights and governance.](#)
10. [Kyoto Protocol Reference Manual on Accounting of Emissions and Assigned Amount, United Nations Framework Convention on Climate Change, 2018.](#)
11. [D. Mihaela, K. Michael, Environmental impact of HFO refrigerants & alternatives for the future, June 2021.](#)
12. [K. Tokuhashi, T. Uchimarū, K. Takizawa, S. Kondo, Rate Constants for the Reactions of OH Radicals with the \(E\)/\(Z\) Isomers of CF₃CF=CHCL and CHF₂CF=CHCL, *The Journal of Physical Chemistry*, 122, 3120-3127, 2018.](#)
13. [Leaflet for refrigerant \(AMOLEA 1224yd\), AGC Chemicals.](#)

14. S. Loreface, M. Sardi, Calibration of a reference vibrating tube densimeter, INRIM, 2012.
15. R. Romeo, P. A. Giuliano Albo, S. Lago, J. S. Brown, Experimental liquid densities of cis-1,3,3,3-tetrafluoroprop-1-ene (R1234ze(Z)) and trans-1-chloro-3,3,3-trifluoropropene (R1233zd(E)), *International Journal of Refrigeration*, 79, 176-182, 2017.
16. C. Bouchot, D. Richon, An enhanced method to calibrate vibrating tube densimeters, *Fluid Phase Equilibria*, 191, 189-208, 2001.
17. W. Wagner, A. Pruss, The IAPWS Formulation 1995 for the Thermodynamic Properties of Ordinary Water Substance for General and Scientific use, *Journal of Physical and Chemical Reference Data*, 31, 387–535, 2002.
18. R. Akasaka, M. Fukushima, E. W. Lemmon, A Helmholtz Energy Equation of State for cis-1-chloro-2,3,3,3-Tetrafluoropropene (R-1224yd(Z)), *European Conference on Thermophysical Properties*, 2017.
19. L. Fedele, S. Bobbo, M. Scattolini, C. Zilio, R. Akasaka, HCFO refrigerant cis-1-chloro-2,3,3,3 tetrafluoropropene [R1224yd(Z)]: Experimental assessment and correlation of the liquid density, *International Journal of Refrigeration*, 118, 139-145, 2020.

9. Appendix

```

1. output_precision(9);
2. global H;
3. global R;
4. global V;
5. global P0;
6. global T0;
7. global N;
8. global M;
9. global Ht;
10. global Hp;
11. global Ho;
12. global Vt;
13. global Vo;
14. global a;
15. global v;
16. global tau_Vo;
17. global d;
18. global X;
19. %global Y;
20. global res_Vo;
21.
22. H=xlsread('water-copia.xlsx');
23. R=xlsread('R1224yd data.xlsx');
24. V=xlsread('vaccum.xlsx');
25. P0=18e-6;
26. P1=1e6;
27. T0=333;
28. %N=2;
29. %M=3;
30.
31. # Refrigerant Data
32. Rt=R(:,1);
33. Rp=R(:,2)*1e6;
34. Ro=R(:,3)*1e-6;
35. Rrowh=R(:,4);
36. Refrow1=R(:,5);
37. Rprop=R(:,6);
38.
39. # Water Data
40. Ht=H(:,1);
41. Hp=H(:,2)*1e6;
42. Ho=H(:,3)*1e-6;
43.
44. # Vaccum Data
45. Vt=V(:,1);
46. Vo=V(:,2)*1e-6;
47.
48. # Period for Vaccum at reference temperatues

```

```

49. v = [(Vt).^0,(Vt).^1,(Vt).^2];
50. a = (inv(v'*v))*v'*Vo;
51. tau_Vo=a(1,1)+a(2,1)*Vt+a(3,1)*Vt.^2;
52.
53. res_Vo=((Vo-tau_Vo)./(tau_Vo))*100;
54. %Vo= a(1,1)+a(2,1)*Vt+a(3,1)*Vt.^2;
55. %v=[Vt.^[0:2]];
56.
57. # period for Water at reference temperatues
58. X=[((Ht-T0).^0).*((Hp-P0).^0) ((Ht-T0).^1).*((Hp-P0).^0) ((Ht-T0).^2).*((Hp-P0).^0) ((Ht-
T0).^3).*((Hp-P0).^0) ((Ht-T0).^0).*((Hp-P0).^1) ((Ht-T0).^1).*((Hp-P0).^1) ((Ht-
T0).^2).*((Hp-P0).^1) ((Ht-T0).^3).*((Hp-P0).^1) ((Ht-T0).^0).*((Hp-P0).^2) ((Ht-
T0).^1).*((Hp-P0).^2) ((Ht-T0).^2).*((Hp-P0).^2) ((Ht-T0).^3).*((Hp-P0).^2)];
59. %3x3 X=[((Ht-T0).^0).*((Hp-P0).^0) ((Ht-T0).^1).*((Hp-P0).^0) ((Ht-T0).^2).*((Hp-P0).^0)
((Ht-T0).^0).*((Hp-P0).^1) ((Ht-T0).^1).*((Hp-P0).^1) ((Ht-T0).^2).*((Hp-P0).^1) ((Ht-
T0).^0).*((Hp-P0).^2) ((Ht-T0).^1).*((Hp-P0).^2) ((Ht-T0).^2).*((Hp-P0).^2) ((Ht-
T0).^3).*((Hp-P0).^0) ((Ht-T0).^3).*((Hp-P0).^1) ((Ht-T0).^3).*((Hp-P0).^2) ((Ht-
T0).^0).*((Hp-P0).^3) ((Ht-T0).^1).*((Hp-P0).^3) ((Ht-T0).^2).*((Hp-P0).^3) ((Ht-
T0).^3).*((Hp-P0).^3)];
60. d = inv(X'*X)*X'*Ho;
61. tau_Ho=X*d;
62.
63. res_Ho=((Ho-tau_Ho)./tau_Ho)*100;
64. %X=[(Ht-T0)'.^[0:M]].*[(Hp-P0)'.^[0:N]];
65. %X=[(Ht-T0).^[0:M]][:[Hp-P0).^[0:N]];
66. %X=[(Ht-T0).^[0:M]];
67. %Y=[(Hp-P0).^[0:N]];
68. %Z=X.*Y;
69. %d=(inv(Z'*Z))*Z'*Ho;
70. %X=[((Ht-T0).^0).*((Hp-P0).^2) ((Ht-T0).^1).*((Hp-P0).^2) ((Ht-T0).^2).*((Hp-P0).^2)];
71. %d=(inv(X'*X))*X'*Ho;
72.
73. # period for Water at 1Mpa
74. %Z=[((Ht-T0).^0).*((Hp-P1).^0) ((Ht-T0).^1).*((Hp-P1).^0) ((Ht-T0).^2).*((Hp-P1).^0) ((Ht-
T0).^3).*((Hp-P1).^0) ((Ht-T0).^0).*((Hp-P1).^1) ((Ht-T0).^1).*((Hp-P1).^1) ((Ht-
T0).^2).*((Hp-P1).^1) ((Ht-T0).^3).*((Hp-P1).^1) ((Ht-T0).^0).*((Hp-P1).^2) ((Ht-
T0).^1).*((Hp-P1).^2) ((Ht-T0).^2).*((Hp-P1).^2) ((Ht-T0).^3).*((Hp-P1).^2)];
75. %e = inv(Z'*Z)*Z'*Ho;
76. %tau_Ho1=Z*e;
77.
78. figure(1);
79. plot(Ht,res_Ho,'k*');
80.
81. % Period of water at the temperature of refrigerant
82. Y=[((Rt-T0).^0).*((Rp-P0).^0) ((Rt-T0).^1).*((Rp-P0).^0) ((Rt-T0).^2).*((Rp-P0).^0) ((Rt-
T0).^3).*((Rp-P0).^0) ((Rt-T0).^0).*((Rp-P0).^1) ((Rt-T0).^1).*((Rp-P0).^1) ((Rt-T0).^2).*((Rp-
P0).^1) ((Rt-T0).^3).*((Rp-P0).^1) ((Rt-T0).^0).*((Rp-P0).^2) ((Rt-T0).^1).*((Rp-P0).^2) ((Rt-
T0).^2).*((Rp-P0).^2) ((Rt-T0).^3).*((Rp-P0).^2)];

```

83. $\tau_{rh} = Y \cdot d;$

84.

85. % Period of water at 1Mpa and Refrigerant temperatures

86. $W = [((Rt - T0)^0 \cdot (P1 - P0)^0) ((Rt - T0)^1 \cdot (P1 - P0)^0) ((Rt - T0)^2 \cdot (P1 - P0)^0) ((Rt - T0)^3 \cdot (P1 - P0)^0) ((Rt - T0)^0 \cdot (P1 - P0)^1) ((Rt - T0)^1 \cdot (P1 - P0)^1) ((Rt - T0)^2 \cdot (P1 - P0)^1) ((Rt - T0)^3 \cdot (P1 - P0)^1) ((Rt - T0)^0 \cdot (P1 - P0)^2) ((Rt - T0)^1 \cdot (P1 - P0)^2) ((Rt - T0)^2 \cdot (P1 - P0)^2) ((Rt - T0)^3 \cdot (P1 - P0)^2)];$

87. $\tau_{rh1} = W \cdot d;$

88.

89. % Period of Vacuum at Refrigerant temperatures

90. $\tau_{avr} = a(1,1) + a(2,1) \cdot Rt + a(3,1) \cdot Rt^2;$

91.

92. % Density calculation of Refrigerant

93. $\text{dens} = (((Ro^2 - \tau_{rh}^2) / (\tau_{rh1}^2 - \tau_{avr}^2)) \cdot \text{Refrow1}) + Rrowh;$

94.

95. $\text{dev} = ((\text{dens} - Rprop) / (Rprop)) \cdot 100;$

96.

97. `figure(2);`

98. `plot(Rt, dev, 'b*')`